*Submillimeter Astrophysics and Technology: A Symposium Honoring Thomas G. Phillips*
*ASP Conference Series, Vol. 417, © 2009*
*D. C. Lis, J. E. Vaillancourt, P. F. Goldsmith, T. A. Bell,*
*N. Z. Scoville, and J. Zmuidzinas, eds.*

# New Results from GISMO, a 2 mm Camera Using a Backshort-Under-Grid TES Bolometer Array

Johannes Staguhn,[1,2] Dominic Benford,[1] Christine Allen,[1] Rick Arendt,[1] Jithin George,[2] Dale Fixsen,[1,2] Stephen Maher,[1] Elmer Sharp,[1] Troy Ames,[1] David Chuss,[1] Eli Dwek,[1] Catherine Marx,[1] Tim Miller,[1] S. Harvey Moseley,[1] Santiago Navarro,[3] Eva Schinnerer,[4] Albrecht Sievers,[3] Fabian Walter,[4] and Edward Wollack[1]

[1]*NASA/Goddard Space Flight Center, Greenbelt, MD 20771, USA*
[2]*University of Maryland, College Park, USA* [3]*IRAM, Granada, Spain,*
[4]*MPIA, Heidelberg, Germany*

**Abstract.** In October 2008, we demonstrated for the second time our 2 mm bolometer camera GISMO (the Goddard IRAM Superconducting 2 Millimeter Observer) for astronomical observations at the IRAM 30 m telescope in Spain. GISMO uses a monolithic $8\times16$ Backshort Under Grid (BUG) array with superconducting Transition Edge Sensors (TES). The instrument's fast beam yields $0.9\lambda/D$ pixel sampling, which optimizes GISMO for detecting sources serendipitously in large sky surveys, while the capability for diffraction limited imaging is preserved. In order to ensure GISMO's operation under all weather conditions, we used a 40% neutral density filter at 4 K. In less than ideal weather conditions we obtained map sensitivities for the working pixels of between 40 mJy $s^{-1/2}$ and 50 mJy $s^{-1/2}$. These numbers are consistent with our atmospheric model calculations. The predicted map NEFDs range from 28 to 56 mJy $s^{-1/2}$ for GISMO's optical configuration (including the 40% neutral density filter) and observing conditions ranging between 10% and 40% line of sight opacities. With an optimized observing strategy for point sources of known position, this sensitivity can further be increased by a factor of 1.5, which we demonstrate by means of analyzing of our signal to noise ratio achieved for point source crossings in the time stream data. The noise in our co-added maps (with few thousand seconds of integration time) scales very well with the square root of time down to sub-mJy levels. We have now designed a cryogenic mechanism that will allow us to move neutral density filters in or out of the beam during future observations. Our simulations indicate that we will gain a factor of 2.4 in observing efficiency if we take out the neutral density filter under good weather conditions. Under typical conditions (20% line of sight sky opacity) we expect to achieve a good pixel map sensitivity of 22 mJy $s^{-1/2}$ and a map NEFD of 1 mJy in an observation lasting about 8 minutes.

## 1 GISMO — a 2 mm Bolometer Camera for the IRAM 30 m Telescope

The 2 mm spectral range provides a unique terrestrial window enabling ground-based observations of the earliest active dusty galaxies in the universe and thereby allowing a better constraint on the star formation rate in these objects (Staguhn et al. 2007a). In order to provide the IRAM 30 m telescope (Baars et al.

1983) with the capability at observing in this important atmospheric window, we have built the Goddard IRAM Superconducting 2 Millimeter Observer GISMO (Staguhn et al. 2006a), which uses a $16 \times 8$ Backshort Under Grid (BUG) array of superconducting Transition Edge Sensors (TES) (Allen et al. 2006; Staguhn et al. 2006b). The optics provide for a 0.9 $\lambda$/D sampling, intended to optimize the efficiency of GISMO for large area blank sky surveys. The Lissajous observing mode provides for diffraction limited angular resolution and reduces correlation times between different regions on the sky.

## 2 Modifications of the GISMO Dewar for Run 2

A number of modifications were implemented in the GISMO instrument to improve on the configuration used during the first observing run in November 2007 (Staguhn et al. 2008). The main modifications were as follows: a stray light problem arising from undersized baffles was eliminated by replacing the old circular baffles with elliptical baffles that tightly enclose the beam (Sharp et al. 2008). The mechanical design of the detector package, which during run 1 led to the detachment of one ceramic board that holds cryogenic readout chips, was revised; the circuit board in the detector package was completely re-designed to prevent a repeat of this problem (Benford et al. 2008). The new board furthermore allowed us to use a more reliable commercially made cold harness. We also completely opto-decoupled all electrical signal lines going into and out of the dewar. Furthermore, we significantly improved the magnetic pickup in the second stage SQUIDs by oversizing the niobium foild under the SQUID multiplexers. In the 30 m cabin we wrapped the dewar stand with eccosorb sheets and the local oscillators in the receiver cabin were turned off by the IRAM staff.

## 3 Results from the Second Observing Run

GISMO was installed on the telescope on Pico Veleta, Spain, for observations beginning Tuesday, 21 October 2008. As was the case during the first observing run, we used a 40% transmission neutral density filter at 4 K in the instrument. This was done to ensure that the detectors would not saturate under any observing conditions. Using the neutral density filter was in particular necessary, since this time we encountered worse weather conditions than in the 2007 observing run.

Due to an internal short in a SQUID multiplexer chip we had to turn off the bias for one quadrant of GISMO's detector array. The yield of working detectors in the other quadrants was more than 80%, however, due to a problem with one connector a few of those pixels were at times up to a factor of 2 noisier than usual, and therefore often were flagged as bad by our data analysis software.

### 3.1 Current Noise Density Spectra

In particular a result of using opto-couplers for all signal lines into the dewar, the detector noise spectra we obtained in the receiver cabin with the dewar window closed are very clean. Figure 1 shows the average of current noise density measurements of 64 detector pixels under different illumination conditions, in all cases with and without common mode subtracted: (1) quasar observations during during mediocre weather, (2) blank sky during good weather, and (3) dewar window blanked off. The relatively poor weather conditions manifested themselves not only in the higher white noise power from the sky at frequencies exceeding 10 Hz (Fig. 1, top spectrum), but are also prominently traced by the fact that the sky noise (arising from temporal variations in the water vapor in the line of sight) has a higher frequency 1/f knee than was observed under the very good conditions during the first observing run (Staguhn et al. 2008).

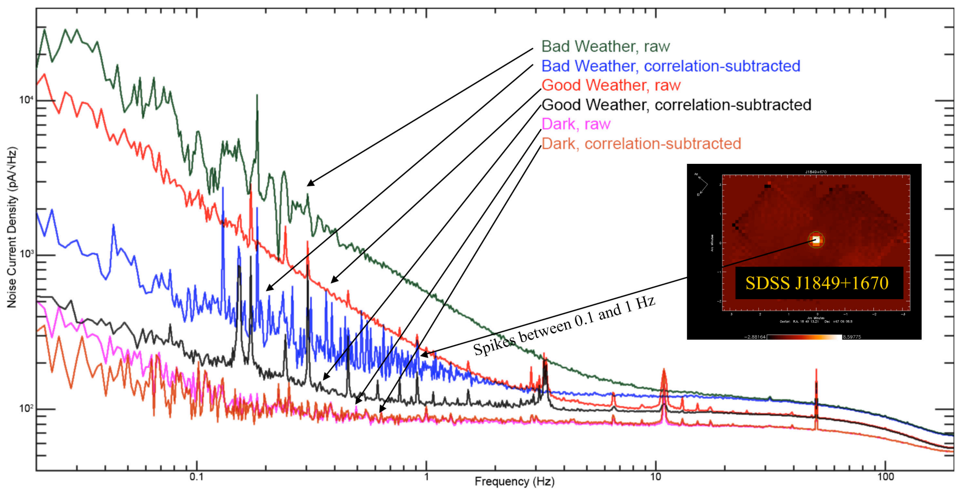


Figure 1. Current noise density spectrum measured for 64 GISMO pixels on the sky under different weather conditions and with the shutter closed as indicated on the labels. Note the quasar's signal in the Lissajous signal band between 0.1 and 1.5 Hz in the bad weather, common mode subtracted spectrum.

Even after common mode subtraction the detected white noise at frequencies $> 10$ Hz in the bad weather data is significantly above the noise floor from the GISMO instrument (i.e., GISMO blanked off). In this case the white noise level in the sky measurement is increased over the dark detector white noise level by more than a factor of $\sqrt{2}$. This means the sky signal exceeds the phonon noise from the detector plus the photon noise from inside the instrument. At lower frequencies the sky 1/f noise becomes dominant. Note that in the common mode subtracted spectrum the quasar SDSS J1849+1670 can be directly seen as spikes in the Lissajous signal band between 0.1 and 1.5 Hz. Under good weather conditions the noise floor from the GISMO instrument is comparable to the white noise level ($\geq 1$ Hz) from the sky. However, our simulations predict that without the 40% neutral density filter, the sky would have dominated under these and even better conditions.

### 3.2 Time Domain Data

In order to verify the noise performance of GISMO with a method that is independent of our map-making procedures, we investigated how the noise in our raw data stream compares to the signal we see from a known source, the quasar 3C545 when it centrally crosses a pixel. The flux from 3C454 is assumed to be

12.5 Jy at 2 mm on the date of those observations. With this flux we derive a noise level of 30 mJy $s^{-1/2}$ in our time stream data, consistent with the predicted noise under 70% sky transmission conditions. These observations were obtained in the same night that the data of J1148+5251 were taken. Clouds were present all night. Note that the derived point source sensitivity of 30 mJy $s^{-1/2}$ in time stream data corresponds to a map point source sensitivity of 42 mJy $Hz^{-1/2}$ for our 0.9 $\lambda/D$ sampled pixels.

### 3.3 Maps of Astronomical Sources

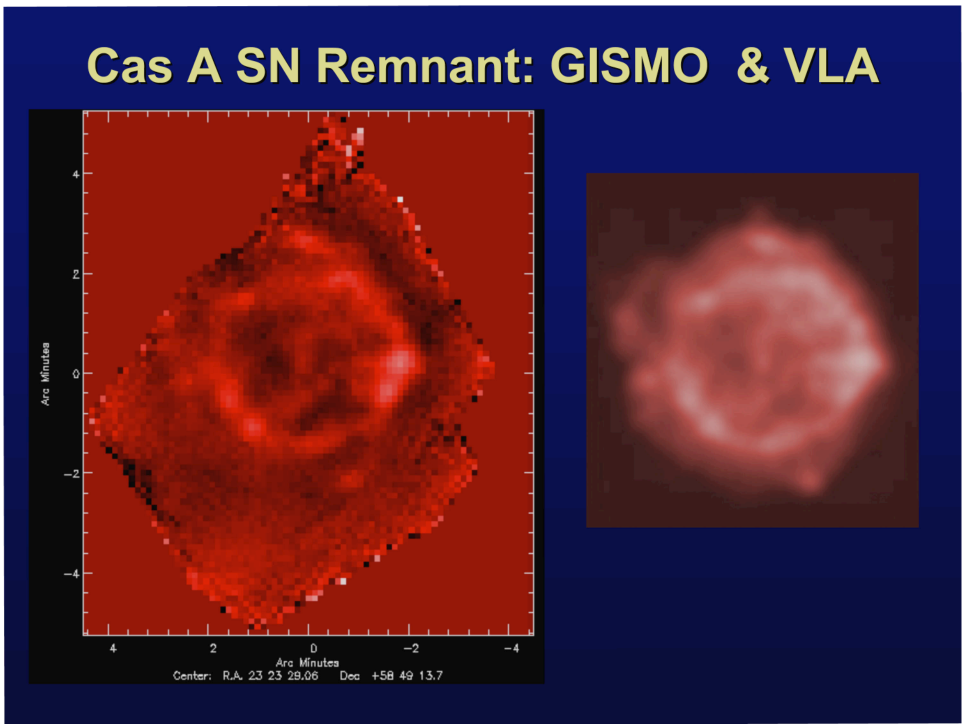


Figure 2. *left:* GISMO observations of the Cas A supernova remnant. *right:* VLA 21 cm observations of Cas A, smoothed to GISMO's angular resolution.

During mostly poor weather condition we typically achieved sensitivities in our maps that correspond to between 40 and 50 mJy $s^{-1/2}$ for the equivalent integration time of all pixels that were flagged as good. These values are consistent with our refined atmospheric efficiency model calculations that predict NEFDs ranging from 28 to 56 mJy $s^{-1/2}$ for GISMO's optical configuration and observing conditions ranging between 10% and 40% line of sight opacities. The noise in our coadded maps (with few thousand seconds of integration time) scales very well to sub-mJy levels with the square root of time. Despite the fact that the bad weather did not allow us to demonstrate integrations well below sub-mJy levels, we were able obtain a significant number of astronomical observations. Examples follow below. Furthermore, the data enabled us to investigate the properties of the atmosphere under rather moderate conditions and to test the ability of our data reduction algorithms for astronomical observations taken

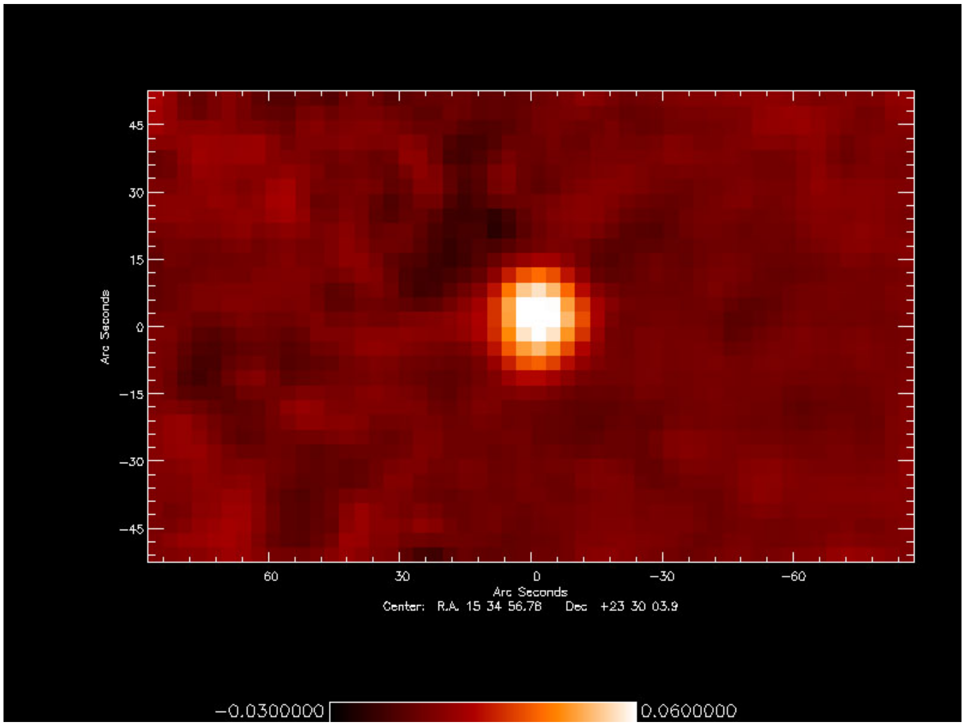


Figure 3. GISMO 2 mm map of Arp220. The displayed units are Jy/beam.

under these conditions. Figure 2 shows a GISMO map of the supernova remnant Cas A, demonstrating our ability to successfully reduce extended source observations, using advanced data reduction techniques. Figure 3 shows the high signal-to-noise GISMO map of the prototypical ULIRG Arp 220 in units of Jy/beam.

## 4 Conclusion and Outlook

All three methods (analysis of current noise density spectra under different loads, time domain point source extraction, and signal to noise in astronomical maps) used to obtain the noise performance of GISMO, yield consistent results. The measured noise levels agree well with our sky noise models. We are currently designing a cryogenic mechanism that will allow us to use one or two neutral density filters only when the sky background requires this. Under good to normal conditions there is no need to use a neutral density filter. This setup will significantly increase the effective dynamic range of our detectors and as a result will allow background limited observations under almost all observing conditions. Our simulations indicate that we will gain a factor of 2.4 in observing efficiency if we take out the neutral density filter.

By now we have replaced the bad SQUID multiplexer, as well as a bad connector. As a result we observe virtually no excess noise in any of the pixels and have now a total pixel yield of more than 90%. With a good pixel yield of 90% we can expect to achieve the same observing efficiency we obtained in run 2 in less than a quarter of the integration time. Under typical conditions (20% line of sight sky opacity) we expect to achieve a good pixel map sensitivity of 22 mJy $s^{-1/2}$ or a map NEFD of 1 mJy in an observation lasting about 8 minutes. With the right observing strategy for point sources of known position, this sensitivity theoretically can further be reduced by a factor of 1.5 (2.3 in observing time).

**Acknowledgments.** This work was supported in part by NSF Grant AST 0705185

### References

Allen, C. A.; Abrahams, J., Benford, D. J., Chervenak, J. A., Chuss, D. T., Staguhn, J. G., Miller, T. M., Moseley, S. H., Wollack, E. J., "Far infrared through millimeter backshort-under-grid arrays", 2006, SPIE, 6265E, 9A

Benford, Dominic J., Staguhn, Johannes G.; Allen, Christine A.; Sharp, Elmer H., "A compact, modular superconducting bolometer array package", 2008, SPIE, 7020, 56

Baars, J. W. M., Hooghoudt, B. G.; Mezger, P. G.; de Jonge, M. J., 1983, A&A, 1785, 319

Sharp, Elmer H.; Benford, Dominic J.; Fixsen, Dale J.; Maher, Stephen F.; Marx, Catherine T.; Staguhn, Johannes G.; Wollack, Edward J., "Design and performance of a high-throughput cryogenic detector system", 2008, SPIE, 7020, 66

Staguhn, J. G.; Benford, D. J.; Allen, C.A.; Moseley, S. H.; Sharp, E. H.; Ames, T. J.; Brunswig, W.; Chuss, D. T.; Dwek, E.; Maher, S. F.; Marx, C. T.; Miller, T. M.; Navarro, S.; Wollack, E. J., "GISMO: a 2-millimeter bolometer camera for the IRAM 30 m telescope", 2006a, SPIE, 6275E, 44S

Staguhn, J.G, Allen, C.A, Benford, D.J., Chervenak, J.A, Chuss, D.T., Miller, T.M., Moseley, S.H., Wollack, E.J., "Characterization of TES bolometers used in 2-dimensional Backshort-Under-Grid (BUG) arrays for far-infrared astronomy", 2006b, Nuclear Instruments and Methods in Physics Research, Section A, 559, 545

Staguhn, J. G.; Dwek, E.; Benford, D. J.; Moseley, S. H.; Sharp, E. H., "Science case for a 2 mm bolometer camera optimized for surveys of dusty galaxies in the high-redshift Universe", 2007, Il Nuovo Cimento B, 122, 1311

Staguhn, J.G.; Benford, D.J.; Allen, C.A.; Maher, S. F.; Sharp, E.H.; Ames, T.J.; Arendt, R.G.; Chuss, D.T.; Dwek, E.; Fixsen, D.J.; Miller, T.M.; Moseley, S. H.; Navarro, S.; Sievers, A.; Wollack, E.J., "Instrument performance of GISMO, a 2 millimeter TES bolometer camera used at the IRAM 30 m Telescope", 2008, SPIE, 7020, 3